Available online at www.sciencedirect.com

ScienceDirect

Procedia Structural Integrity 54 (2024) 307–313

Structural Integrity Procedia

www.elsevier.com/locate/procedia

International Conference on Structural Integrity 2023 (ICSI 2023)

On the use of uniaxial one-parameter damage laws for estimating fatigue life under multiaxial loading

R. Branco[a,*], J.D. Costa[a], L.P. Borrego[b,a], Z. Marciniak[b], W.Macek[c], F. Berto[d]

[a]*CEMMPRE, Department of Mechanical Engineering, University of Coimbra, Rua Luis Reis Santos, 3030-788 Coimbra, Portugal*
[b]*Polytechnic University of Coimbra,, Coimbra Institute of Engineering, Department of Mechanical Engineering, Rua Pedro Nunes - Quinta da Nora,, 3030-199 Coimbra, Portugal*
[c]*Opole University of Technology, Department of Mechanics and Machine Design, Opole, Poland*
[d]*Gdansk University of Technology, Faculty of Mechanical Engineering and Ship Technology, Gdansk 80-233, Poland*
[e]*Department of Chemical Engineering Materials Environment, Sapienza - Università di Roma, 00184 Roma, Italy*

Abstract

The goal of this paper is to evaluate the capabilities of different one-parameter fatigue laws to estimate crack initiation in notched components under multiaxial loading. Fatigue damage is accounted for through stress-based, strain-based, and energy-based approaches while the cyclic plasticity at the notch-controlled process zone is estimated using linear-elastic simulations. The results show that energy-based formulations established from both the absorbed energy at the mid-life cycle and the energy absorbed throughout the entire life are more accurate.

Keywords: Multiaxial fatigue, uniaxial one-parameter fatigue laws, crack initiation

1. Introduction

Fatigue life assessment of mechanical components experiencing multiaxial loading is a complex challenge. In part, this is because there is a huge number of variables involved in the analysis, namely the shape of the stress

* Corresponding author. Tel.: +351 239 790 700; fax: +351 239 403 407.
E-mail address: Ricardo.branco@dem.uc.pt

10.1016/j.prostr.2024.01.088

Nomenclature

b	fatigue strength exponent
c	fatigue ductility exponent
E	Young's modulus
N_f	number of cycles to failure
N_E	experimental fatigue life
N_P	predicted fatigue life
W_T	cumulative total strain energy density
ΔW_{T0}	tensile elastic energy at the material fatigue limit
ΔW_T	total strain energy density at mid-life
α	material constant
α_t	material constant
ε_a	strain amplitude
ε_f'	fatigue ductility coefficient
κ	material constant
κ_t	material constant
σ_a	stress amplitude
σ_f'	fatigue strength coefficient
σ_m	mean stress
σ_{max}	maximum stress

raiser, the normal stresses to shear stresses ratio, the loading orientation with respect to the notch configuration, among others (Socie and Marquis, 1999). The unlimited number of variables increases the difficulty and introduces some unpredictability. Thus, there is a need for unified models capable of accounting for the fatigue damage at the critical points in an accurate manner (Carpinteri et al., 2008; Zhu et al. 2020; Deng et al., 2022).

Within the most successful approaches to assess the multiaxial fatigue life of notched components, the idea of reducing the multiaxial state to an equivalent uniaxial state is one of the most popular (Carpinteri et al., 2011; Branco et al., 2017). These approaches can be established through stress-based, strain-based, or energy-based parameters. These parameters, frequently named as fatigue damage quantifiers, can be determined simply by an average value computed near the notch tip or using more complex concepts, such as weighted methods (Susmel and Taylor, 2007; Liao et al, 2020).

The Theory of Critical Distances (TCD) and the Strain Energy Density (SED) are two popular average methods. The former owes its success to the balance between simplicity and accuracy. Although the first formulations have been established using stress concepts (Susmel and Taylor, 2007; Ellyin, 1997), modern approaches also consider strain and energy quantities. Regarding the latter, its popularity relies on the possibility of dealing with a variety of problems and loading scenarios. However, comparative studies focused on both methodologies are not frequent (Hu et al., 2019; Branco et al., 2022).

Both methodologies can be formalised using elastic-plastic and linear-elastic simulations. Despite elastic-plastic analyses are, in theory, more accurate, linear-elastic analyses are simpler and faster because they do not require complex constitutive models. However, comparative studies on the capabilities of each approach rarely have been addressed in literature (Susmel, 2021; Branco; 2021). Thus, the main purpose of this paper is to evaluate the capabilities of TCD and SED approaches combined with different uniaxial one-parameter fatigue laws materialized in a linear-elastic framework for estimating the crack initiation life in notched components under multiaxial loading.

2. Material and methods

The material utilized in this study is the DIN 34CrNiMo6 high-strength steel. Experimental tests comprised both low-cycle fatigue (LCF) testes for evaluation of cyclic fatigue properties (see Table 1) and multiaxial fatigue tests

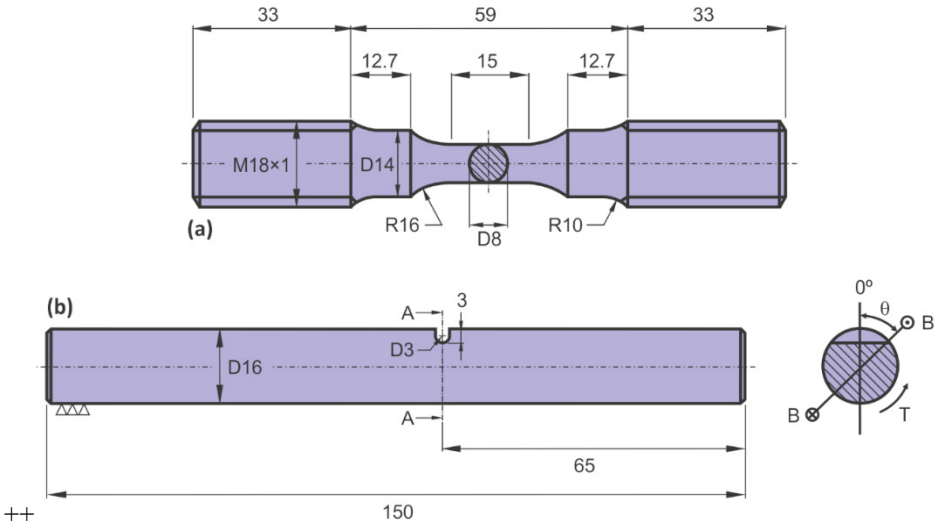

Fig. 1. Specimen geometries: (a) low-cycle fatigue tests; and (b) multiaxial bending-torsion fatigue tests (unit: mm).

Table 1. Cyclic fatigue properties of the 34CrNiMo6 high-strength steel.

σ_f' (MPa)	b	ε_f'	c	κ_t (MJ/m^3)	α_t	ΔW_{t0} (MJ/m^3)	κ (MJ/m^3)	α
1183.7	-0.0545	0.4697	-0.6059	2165.37	-0.6854	0.7049	1022.62	0.356

Table 2. Summary of multiaxial fatigue tests.

Test	B/T	θ	σ_a (MPa)	σ_m (MPa)	τ_a (MPa)	τ_m (MPa)	N_i (cycle)
1	2	0º	179.1	194.0	44.9	48.5	102,386
2	2	0º	223.8	238.7	56.0	59.7	49,103
3	2	0º	298.4	313.3	74.6	78.3	24,207
4	2	45º	208.9	223.8	52.2	56.0	64,754
5	2	45º	253.7	268.6	63.4	67.2	39,331
6	2	45º	328.3	343.2	82.1	85.8	11,422
7	2	90º	343.0	365.3	85.8	91.3	68,010
8	2	90º	356.4	383.1	89.1	95.8	72,072
9	2	90º	364.1	379.0	91.0	94.8	51,878
10	1	0º	179.1	194.0	89.6	97.0	92,544
12	1	0º	179.1	194.0	89.6	97.0	83,278
13	1	0º	179.1	194.0	89.6	97.0	56,749
14	1	0º	223.8	238.7	112.0	119.4	26,420
15	1	0º	223.8	238.7	112.0	119.4	21,225
16	1	0º	223.8	238.7	112.0	119.4	31,306
17	1	0º	298.4	313.3	149.2	156.7	8314
18	1	45º	208.9	223.8	104.5	111.9	67,160
19	1	45º	223.8	238.7	111.9	119.4	46,822
20	1	45º	238.7	253.7	119.4	126.9	25,276
21	1	90º	282.9	298.5	141.5	149.3	63,105
22	1	90º	283.5	298.4	141.8	149.2	88,655
23	1	90º	311.8	334.1	155.9	167.0	28,730

for calculating the crack initiation life. As far as the LCF tests are concerned, they were performed under uniaxial strain-controlled conditions using standard smooth specimens, see Fig. 1(a), with strain amplitudes (ε_a) in the range 0.5-2-0% and a strain ratio equal to -1 (Branco et al., 2012). In relation to the multiaxial fatigue tests, they were

performed under stress control mode, with a stress ratio equal to 0, considering proportional bending-torsion loading and the notched geometry presented in Fig. 1(b). The loading cases included three relations between the normal stress and the shear stress and three different orientations of the normal stress with respect to the notch root (Branco et al., 2017). Details about the applied stress level and the corresponding values of crack initiation life can be seen in Table 2. Crack initiation life was calculated for a crack size equal to the material characteristic length (a_0). For the material under investigation, for a stress ratio of 0, a_0 was equal to 129 μm (Branco et al., 2017).

The uniaxial one-parameter damage laws analysed in this work included stress-based, strain-based, and energy-based approaches. Regarding the stress-based approaches, it was used the well-know Basquin model:

$$\sigma_a = \left(\sigma_f' - \sigma_m\right)\left(2N_f\right)^b \tag{1}$$

where σ_f' is the fatigue strength coefficient, b is the fatigue strength exponent, σ_m is the mean stress, and N_f is the fatigue life. Concerning the strain-based approaches, it was selected the Coffin-Manson (CM) model:

$$\varepsilon_a = \frac{\left(\sigma_f' - \sigma_m\right)}{E}\left(2\mathrm{N_f}\right)^b + \varepsilon_f'\left(2\mathrm{N_f}\right)^c \tag{2}$$

where ε_f' is the fatigue ductility coefficient, c is the fatigue strength exponent, and E is Young's modulus. In relation to the energy-based approaches, two alternative models were used, namely the total strain energy density (TSED):

$$\Delta \mathrm{W}_t = \kappa_t\left(2\mathrm{N_f}\right)^{\alpha_t} + \Delta W_{0t} \tag{3}$$

and the cumulative total strain energy density (cTSED):

$$\mathrm{W_T} = \kappa\left(N_f\right)^{\alpha} \tag{4}$$

where κ_t, α_t , κ and α are material constants obtained from experimental results, and ΔW_{0t} is the tensile elastic energy at the material fatigue limit. The total strain energy density was calculated from the mid-life cycle while the cumulative total strain energy density was calculated from all cycles. Note that the total strain energy density was calculated by summing both the plastic and the elastic positive components of the stress-strain hysteresis loop.

All the above-mentioned quantities were calculated at the notch region by applying the Line Method (LM) of the TCD over a straight line emanating from the crack initiation site of the notch root. The crack initiation site was defined as the node with maximum value of the first principal stress. This criterion has been successfully validated in previous studies for proportional bending-torsion loading (Branco et al., 2017). The cyclic plasticity at the notch-controlled process zone was simulated using linear-elastic finite-element simulations along with the Equivalent Strain Energy Density concept (Branco et al., 2021).

3. Results and discussion

For each loading case, the multiaxial stress state was reduced to an equivalent uniaxial stress state. This task was carried out by using the stress and strain fields simulated numerically assuming a linear elastic framework combined with the ESED concept (Branco et al., 2021). Then, from the stress-distance, strain-distance, and energy-distance relationships determined over a straight line emanating from the notch root, the LM of the TCD was used to estimate an effective value of the tested quantities, namely an effective value of stress amplitude (Eq. (1)), an effective value of strain amplitude (Eq. (2)), an effective value of total stain energy density (Eq. (3)), and an effective value of cumulative total strain energy density (Eq. (4)).

Figure 2 shows the typical results obtained for the different bending-torsion fatigue tests using the: Basquin model (Fig. 2(a)), the CM model (Fig. 2(b)), the TSED model (Fig. 2(c)), and the cTSED model (Fig. 2(d)). For the sake of comparability, scatter bands with factors of two were also displayed, represented by the dashed straight lines.

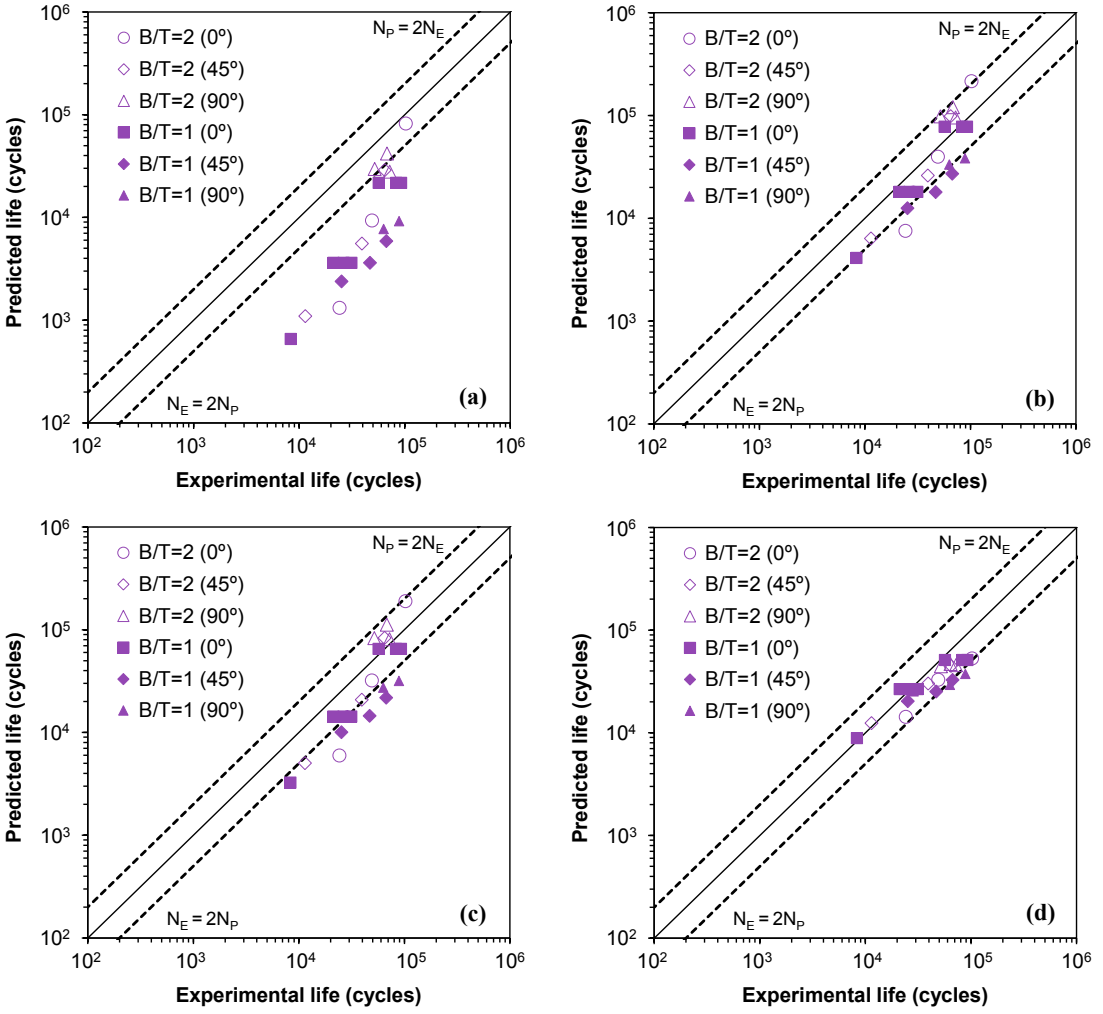

Fig. 2. Fatigue life prediction: (a) stress-based; (b) strain-based; (c) total strain energy density; and (d) cumulative strain energy density.

Overall, as shown in the figure, the predictive capabilities associated with each model are relatively different. In the case of the stress-based approach (see Fig. 2(a)), the results do not correlate well with the experimental fatigue lives for lower lives but are in line for higher fatigue lives. Stress-based approaches are generally more suitable for the high-cycle fatigue regime, which may explain these trends. As far as the strain-based approach is concerned, see Fig. 2(b), the quality of predictions was increased in the entire range. A close analysis of the figure demonstrates that the data are much closer to the scatter bands and the number of points within this delimited region is significantly higher than in the previous case. Strain-based approaches are more adequate to deal with problems in which the fatigue process is governed by cyclic plasticity. This behaviour is also confirmed in this work.

Concerning the energy-based approaches, as described above, two alternative models were considered. Figure 2(c) plots the fatigue life predictions against the experimental lives for the TSED model. In this case, the relationship between the loading level and the fatigue durability is expressed using the mid-life cycles under uniaxial strain-controlled conditions (Branco et al., 2021). It is clear that this model leads to better fatigue life predictions than the other two. In fact, all points are within the scatter bands, and are placed either in the conservative side or in the non-conservative side. Moreover, there are no significant differences for the low-cycle fatigue regime or the high-cycle fatigue regime. Finally, Fig. 2(d) exhibits the fatigue life results for the cumulative strain energy density model. In

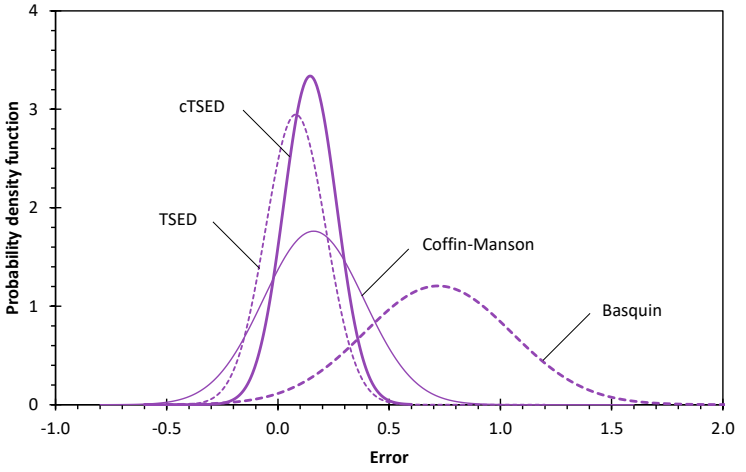

Fig. 3. Probability density functions for the: (a) stress-based; (b) strain-based; (c) total strain energy density; and (d) cumulative strain energy density.

this case, unlike the previous energy-based model, the relationship between the loading level is accounted for by summing the total strain energy density absorbed throughout the entire lifetime, i.e. by accounting for the so-called fatigue toughness (Branco et al., 2022). Similar to the previous case, the cTSED model also led to very good results for the entire range. Nevertheless, in this case, the results were more conservative, which can be attractive from a perspective of fatigue design. On the other hand, it is clear that the results are in a narrow region, which may suggest higher correlation between the applied loading level and the associated fatigue life than in the previous models.

In order to better compare the quality of fatigue life predictions of all tested models, the probability density functions of the fatigue error, defined by the following expression, were calculated:

$$E_N = \text{Log } N_E - \text{Log } N_P \quad (5)$$

where N_E represents the experimental fatigue life, and N_P represents the predicted fatigue life. As shown in Fig. 3, the two energy-based models led to mean errors close to zero and lower standard deviations, which is in line with the results exhibited in Fig. 2. Comparing both energy-based approaches, it can be seen that the cTSED is slightly more conservative, since its probability density function is moved to the right-hand side, and results in lower predictive errors. By contrast, both the stress-based and the strain-based models were less accurate for this notched geometry under the tested loading scenarios.

4. Conclusions

This paper compared the predictive capabilities of the different one-parameter fatigue laws to estimate the crack initiation life in notched components under bending-torsion loading, namely stress-based, strain-based, and energy-based models. Different relations between the normal stress and the shear stress and different loading orientations with respect to the notch root were studied. The following conclusions can be drawn:

- The stress-based approach was not suitable to correlate the applied loading level with the crack initiation life in the low-cycle fatigue regime. In the high-cycle fatigue regime, the results were well correlated;
- The strain-based approach led to better correlations than the stress-based approach, either in the low-cycle fatigue regime or in the high-cycle fatigue regime, but most of results were non-conservative;
- The two energy-based models exhibited good predictive capabilities in the LCF and HCF ranges. The TSED exhibited the lowest mean errors, while the cTSED exhibited the lowest standard deviations.

Acknowledgements

This research is sponsored by FEDER funds through the program COMPETE – Programa Operacional Factores de Competitividade – and by national funds through FCT – Fundação para a Ciência e a Tecnologia – under the project UIDB/00285/2020.

References

Branco, R., Costa, J.D., Antunes, F.V., 2012. Low-cycle fatigue behaviour of 34CrNiMo6 high strength steel. Theoretical and Applied Fracture Mechanics 58, 28-34.

Branco, R., Costa, J.D., Berto, F., Antunes, F.V., 2017. Effect of loading orientation on fatigue behaviour in severely notched round bars under non-zero mean stress bending-torsion. Theoretical and Applied Fracture Mechanics 92, 185-197.

Branco, R., Costa, J.D., Borrego, L.P., Berto, F., Razavi, S.J.M, Macek, W., 2021. Comparison of different one-parameter damage laws and local stress-strain approaches in multiaxial fatigue life assessment of notched components. International Journal of Fatigue 151, 106405.

Branco, R., Martins, R.F., Correia, J.A.F.O., Marciniak, Z., Macek, W., Jesus, J., 2022. On the use of the cumulative strain energy density for fatigue life assessment in advanced high-strength steels. International Journal of Fatigue 164, 107121.

Carpinteri, A., Spagnoli, A., Vantadori, S., Viappiani, D., 2008. A multiaxial criterion for notch high-cycle fatigue using a critical-point method. Eng Fract Mech 75, 1864–1874.

Carpinteri., A., Spagnoli, A., Vantadori, S., 2011. Multiaxial fatigue assessment using a simplified critical plane-based criterion. International Journal of Fatigue 33, 969–976.

Deng, Q.Y., Zhu, S.P., He, J.C., Li, X.K., Carpinteri, A., 2022. Multiaxial fatigue under variable amplitude loadings: Review and solutions. International Journal of Structural Integrity 13, 349-393.

Ellyin, F., 1997. Fatigue Damage, Crack Growth and Life Prediction, Chapman & Hall, London.

Hu, Z., Berto, F., Hong, Y., Susmel, L., 2019. Comparison of TCD and SED methods in fatigue lifetime assessment. International Journal of Fatigue 123, 105–134.

Liao, D., Zhu, S.P., Correia, J.A.F.O., De Jesus, A.M.P., Berto, F, 2020. Recent advances on notch effects in metal fatigue: A review. Fatigue and Fracture of Engineering Materials and Structures 43, 637-659.

Socie, D., Marquis, G. Multiaxial fatigue. SAE International; 1999. ISBN 978-0768004533.

Susmel, L., Taylor, D., 2007. A novel formulation of the theory of critical distances to estimate lifetime of notched components in the medium-cycle fatigue regime. Fatigue and Fracture of Engineering Materials and Structures 30, 567–581.

Zhu, S.P., He, J.C., Liao, D., Wang, Q., Liu, Y., 2020. The effect of notch size on critical distance and fatigue life predictions. Materials and Design 196, 109095.